Shell structure of collective states in ^{56}Fe, ^{58}Fe, and ^{60}Fe

J. B. McGrory and S. Raman
Physics Division, Oak Ridge National Laboratory, Oak Ridge, Tennessee 37830
(Received 17 April 1979)

Conventional shell-model calculations of the iron isotopes with $A = 56$–60 are discussed. The calculated level spectra are in good agreement with experiment. The calculations of $E2$ observables are in reasonable agreement with experiment when added effective charges of 1.0e are used for both neutrons and protons. The neutron effective charge is significantly different from one appropriate (1.9e) for ^{56}Ni. There is a strong state dependence in the effective $M1$ operator, and calculations of $M1$ observables are in general disagreement with experiment. An analysis of the structure of ground-state bands and yrast levels is made in terms of a simple rotational model. In all even isotopes, the intrinsic quadrupole moments in the ground-state "band" shrink dramatically with increasing J. There is evidence of a band crossing in all three even isotopes, but no evidence is found for an abrupt shape change in the ground-state bands of these nuclei. It is concluded that no simple rotational model gives a good description of the low-lying states of the iron isotopes.

[NUCLEAR STRUCTURE ^{56}Fe, ^{57}Fe, ^{58}Fe, ^{59}Fe, ^{60}Fe, calculated levels. ^{56}Fe, ^{58}Fe, ^{60}Fe, calculated $B(M1)$, $B(E2)$, μ, branching ratios. Shell model, Vervier interaction, Horie-Ogawa interaction, effective operators. Comparison with experiment and rotational model.]

I. INTRODUCTION

Among the earliest "large" shell-model calculations[1,2] were those of the isotopes ^{56}Fe, ^{57}Fe, and ^{58}Fe. In those calculations, energy levels and some spectroscopic factors for one- and two-neutron transfer reactions were calculated, and the results were compared with experiment. No investigation of electromagnetic observables was made at that time. Since then, a significant body of new experimental information on energy levels, branching ratios, lifetimes, and reduced transition probabilities has been reported on the isotopes $^{56-58}$Fe, as well as on ^{59}Fe and ^{60}Fe. In particular, there has been considerable interest[3,4] in the structure of the high-spin states in these nuclei. Also, several papers[5-8] discuss the possible existence of an abrupt shape change between ^{56}Fe and ^{58}Fe. Because of the experimental activity in this region, it is useful to extend the shell-model calculations to the high-spin states, to calculate the electromagnetic observables in all the isotopes from ^{56}Fe and ^{60}Fe, to see how well such data can be correlated by the shell model, and to investigate the question of the shape change in these nuclei. In Section II, the model we use is discussed and compared with other models for this same region. In Section III, the calculated energy levels are compared with experiment. In Section IV, the calculation of electromagnetic observables is discussed. The effective transition operators are defined there, and calculated results are compared with experimental results. In Section V, the structure of these isotopes is discussed in terms of bands. The findings are summarized in Section VI.

II. DISCUSSION OF THE MODEL

The calculations reported here are all made in the framework of the conventional shell model. The same model was used in previous calculations[1,2] of the $^{56-58}$Fe isotopes. An inert ^{48}Ca core is assumed. The six protons are restricted to the $0f_{7/2}$ shell. The active neutron space includes the $1p_{3/2}$, $0f_{5/2}$, and $1p_{3/2}$ orbits. The effective Hamiltonian is then, in obvious notation,

$$H = H_{pp} + H_{nn} + H_{pn} + H_{p\text{-core}} + H_{n\text{-core}}.$$

There are four matrix elements of H_{pp} in this model space involving the $|f_{7/2}^2\ J\rangle$ state. The matrix elements are chosen to be 0, 1.41, 2.55, and 2.97 MeV for the J=0, 2, 4, and 6 states, so as essentially to reproduce the observed[9] low-lying states of ^{54}Fe within this same model space. $H_{p\text{-core}}$ is set = 0, since we treat only excitation energies, and there is only one proton orbit in the calculation. $H_{n\text{-core}}$, the neutron single-particle energies, are taken from the observed single-particle states in ^{49}Ca, i.e.,

$$\varepsilon_{3/2} = 0,\ \varepsilon_{1/2} = 2.07, \text{ and } \varepsilon_{5/2} = 3.96.$$

H_{pn} is taken from the work of Vervier.[10] He assumed a delta function force for H_{pn}, and adjusted the force strengths to reproduce the spectrum of ^{57}Ni in the shell-model space we use here, i.e.,

$$\varepsilon_{3/2} = 0,\ \varepsilon_{5/2} = 0.80, \text{ and } \varepsilon_{1/2} = 1.06.$$

For H_{nn} we use a neutron interaction determined by Cohen et al.[11] They treated the isotopes of Ni in a space where a closed ^{56}Ni core is assumed and neutrons occupy the same orbits as are included in the model space used here. The nickel isotopes are fit with an r.m.s. deviation of $\approx$250 keV, so the calculations reported here have an error of that order because of uncertainties in the n-n space. (The n-n interaction we used was obtained from S. Cohen prior to the Cohen et al., publication. Some matrix elements differ by $\approx$10 keV from the published matrix elements.)

Thus, the effective shell-model Hamiltonian is essentially taken from the literature and used without change in these calculations. Within the model

space defined here, all allowed states of all possible configurations are included. The calculations are made with the Oak Ridge-Rochester shell model computer programs.[12]

Horie and Ogawa[13] and Bendjaballah[7] have also calculated ^{56}Fe levels in the same model space as that used here but with a different interaction, viz., an interaction designed by Horie and Ogawa.[13] Their interaction differs in two ways: First, they use a Z-dependent H_{pp}. For each Z value, they identify as "pure $f_{7/2}$ Z-20 states" a selected set of states in the observed spectra of nuclei with the same Z, but with the closed neutron shell at N = 28. The observed eigenvalues are used to specify the matrix elements $\langle \psi^{Z-20} | H_{pp} | \psi^{Z-20} \rangle$. Thus, they do not obviously use a two-body, proton-proton interaction. Since we limit ourselves to the two-proton hole case, there is no difference in H_{pp} in the two calculations. The second difference is that Horie and Ogawa treat the 20 two-body matrix elements of H_{pn} in the model space as free parameters which are adjusted to fit observed spectra of low-lying states in N = 29, Z = 22-26 nuclei. We have used the Horie-Ogawa interaction in the $^{56-58}$Fe calculations, and will cite some results in the next section. The Horie-Ogawa interaction gives quantitatively superior results for the low-lying states of ^{56}Fe. (For observed states in ^{56}Fe below 3.50 MeV, the r.m.s. deviation between theory and experiment is 211 keV for the Horie-Ogawa interaction and 255 keV for the Vervier interaction.) This feature does not persist for ^{57}Fe and ^{58}Fe, so we have not continued such a comparison to ^{59}Fe and ^{60}Fe. We defer discussion of the effective electromagnetic operators until we discuss the calculation of electromagnetic observables.

III. CALCULATED SPECTRA OF THE ISOTOPES ^{56}Fe - ^{60}Fe

The calculated spectra of excited states in the nuclei $^{56-60}$Fe are shown in Figs. 1-5. Also shown in these figures are the observed spectra of these nuclei.[14] In Figs. 1-3 we show also the spectra calculated with the Horie-Ogawa interaction discussed above.

A. Levels in ^{56}Fe

Figure 1 shows the calculated spectra for all positive parity states with $J \leq 6$ up to 5 MeV excitation, plus the two 8^+ states below 6 MeV. In addition to these states, there are high-spin states with $J^\pi = 9^+$ at 7.07 and 8.49 MeV in the calculated spectrum, and states with $J^\pi = 10^+$ at 8.06 and 10.27 MeV. There are no known candidates for these calculated 9^+ and 10^+ states in the observed spectrum. In the observed spectrum, all known positive parity levels below 4.74 MeV are shown, as well as two candidates for 8^+ states. As mentioned above, there is an error of 200-250 keV intrinsic to the present calculation because of uncertainties in the n-n interaction. Within these errors, there are reasonable analogs for all observed positive parity states below 4.0 MeV. There is also good agreement for the 7^+ and 8^+ high-spin states. As for a comparison between the Vervier and Horie-Ogawa interactions, for the lowest six or seven levels, the Horie-Ogawa interaction yields quantitatively superior results than the Vervier interaction. Above 3.2 MeV, the quality of fits is quite comparable,

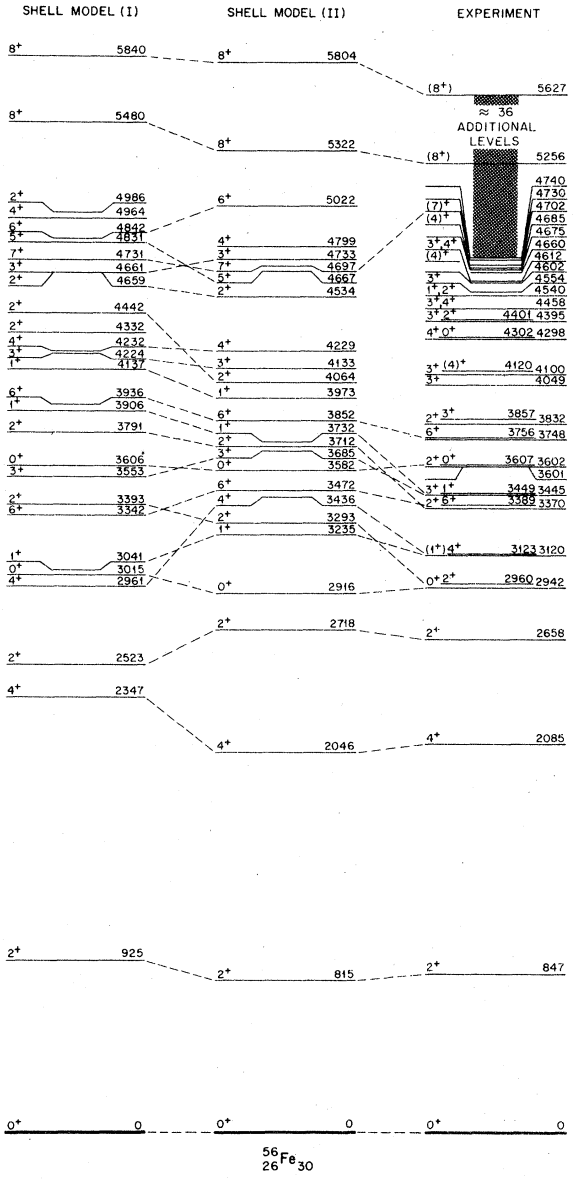

FIG. 1. Comparison between calculated and experimentally known (Ref. 14) energy levels in ^{56}Fe. Shell model (I) refers to the use of the Vervier interaction and shell model (II) to the Horie-Ogawa interaction. All energies are in keV. Dashed lines connect several analogous states.

so that the superiority of the Horie-Ogawa interaction does not persist beyond the lowest levels in ^{56}Fe.

B. Levels in ^{57}Fe

In Fig. 2 all calculated levels up to the highest calculated level for ^{57}Fe are shown for both the Vervier and the Horie-Ogawa interactions. All observed negative parity levels up to the 2.697 MeV,

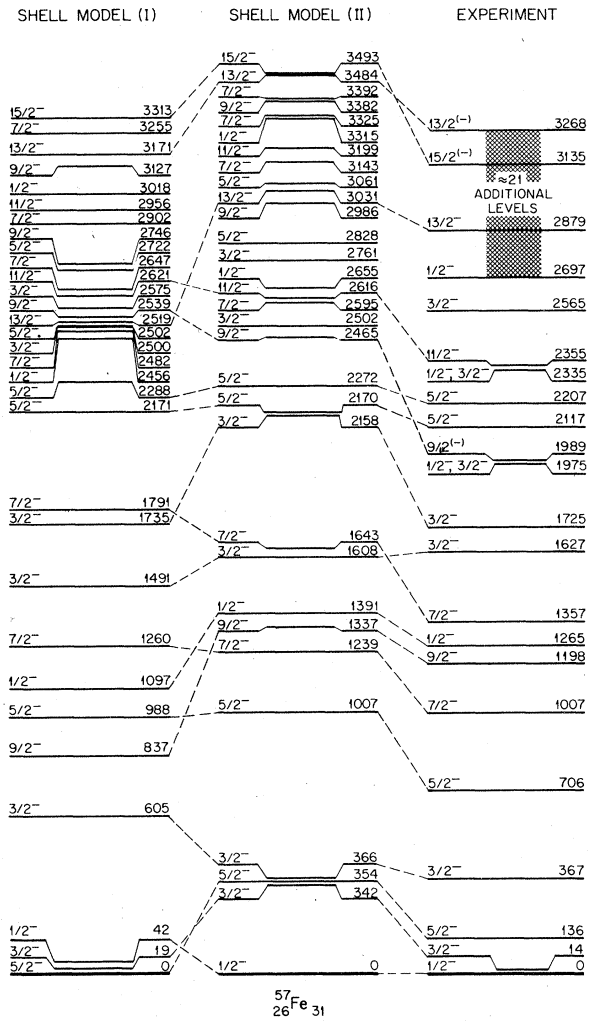

FIG. 2. Comparison between calculated and experimentally known (Ref. 14) energy levels in ^{57}Fe. Shell model (I) refers to the use of the Vervier interaction and shell model (II) to the Horie-Ogawa interaction. All energies are in keV. Dashed lines connect several analogous states.

$1/2^-$ level are shown, as well as the three known high-spin states. Because of the highly expanded energy scale, the theory-experiment discrepancies appear somewhat more significant than for the even isotopes. In fact, for both calculations (Vervier and Horie-Ogawa), the r.m.s. deviation between theory and experiment for the lowest 11 states in the observed spectrum is about 230 keV, close to the already-recognized error in the n-n interaction. The Vervier interaction gives a ground state triplet in agreement with experiment, while the Horie-Ogawa interaction does better for some of the excited states. For the high-spin states with $J^\pi = 13/2^-$ and $15/2^-$, there is again little qualitative difference between the two calculated spectra or between the calculated spectra and the measured one. There are calculated states with spin J = 17/2 - 23/2 for the two interactions at the energies (in MeV) given in Table I. There is no experimental information available on the position of these high-spin states.

C. Levels in ^{58}Fe

In Fig. 3, the spectrum of positive parity states observed below 4.444 MeV is shown, as well as the position of the 7^+ and 8^+ states at 4.668 and 5.340 MeV, respectively. In the calculated spectrum of states labeled Shell Model (I), the Vervier interaction, all states calculated below 4.43 MeV are shown, and also states with $J \geq 6$ which lie below 5.30 MeV. For the Horie-Ogawa interaction, all states calculated below 4.46 MeV are shown, except for the 2^+ and 4^+ states, where only the lowest six states are shown. In addition, in this calculated spectrum, all states with $J \geq 6$ below 5.25 MeV are shown. The theory-experiment agreement here is exceptionally good, better than can be expected from the input. For the Vervier interaction, the r.m.s. deviation between theory and experiment for all observed states below 3.63 MeV for which plausible experimentally-based spin assignments are available is 161 keV. For the Horie-Ogawa interaction, it is 181 keV. There are high-spin states in the calculations for which experimental analogs are not yet known. The calculated excitation energies (in MeV) of the lowest two states for all allowed J values greater than 6 are listed in Table II. Thus, the structure of the calculated spectra of high-spin states is very similar for the Vervier and for the Horie-Ogawa interaction.

D. Levels in ^{59}Fe

The spectrum of observed negative parity states in ^{59}Fe is shown in Fig. 4, as is the spectrum of states calculated with the Vervier interaction. In this case, and for ^{60}Fe, we used only one interaction since the differences between the results calculated with the Horie-Ogawa and Vervier interactions in $^{56-58}$Fe are not qualitatively different. For ^{59}Fe and ^{60}Fe the matrices are large enough that the calculations become costly. It is difficult to make any theory-experiment comparisons for ^{59}Fe because of a lack of firm spin assignments. To date, there is also little information on high-spin states. For completeness, the lowest two calculated excitation energies (in MeV) for all possible spins $J \geq 15/2$ are listed in Table III.

TABLE I. Calculated energies (in MeV) of high-spin states in ^{57}Fe.

J^π	Vervier	Horie-Ogawa	J^π	Vervier	Horie-Ogawa
$17/2^-$	4.26	4.70	$21/2^-$	6.95	6.83
	4.87	5.00		7.43	7.58
$19/2^-$	5.74	5.93	$23/2^-$	8.70	8.80
	6.38	6.49			

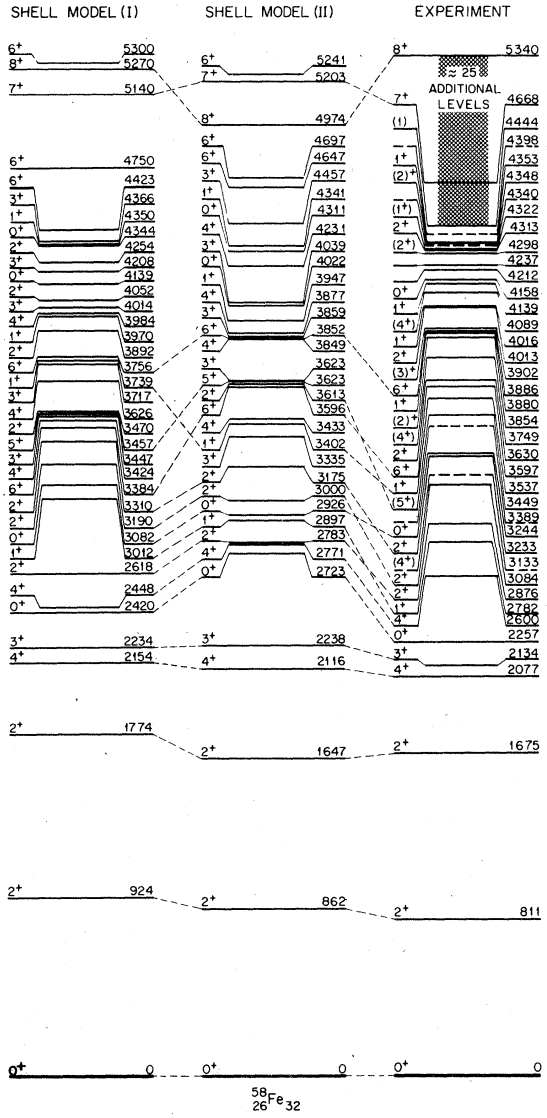

FIG. 3. Comparison between calculated and experimentally known (Ref. 14) energy levels in ^{58}Fe. Shell model (I) refers to the use of the Vervier interaction and shell model (II) to the Horie-Ogawa interaction. All energies are in keV. Dashed lines connect several analogous states.

E. Levels in ^{60}Fe

The calculated and observed spectra of ^{60}Fe are shown in Fig. 5. All known positive parity states below 4.36 MeV are shown, and all states calculated below 4.47 MeV. The theory-experiment agreement is satisfactory for states observed below 3 MeV if the two states which are suggested at 1.67 and 1.88 MeV are actually not there. These states were proposed from a study of the ^{48}Ca(^{18}O,α2nγ) reaction.[15] Referring to Fig. 5, there are not enough spin assignments for levels above 3 MeV in the experimental spectrum to permit any believable comparisons. We list in Table IV the lowest two calculated excitation energies (in MeV) for spins $J \geq 6$ in ^{60}Fe.

TABLE II. Calculated energies (in MeV) of high-spin states in ^{58}Fe.

J^π	Vervier	Horie-Ogawa	J^π	Vervier	Horie-Ogawa
7^+	5.14	5.20	10^+	7.12	7.26
	5.50	5.55		7.72	7.78
8^+	5.27	4.97	11^+	8.52	8.46
	5.39	5.66		10.09	9.97
9^+	6.40	6.54	12^+	9.86	9.75
	6.94	6.95		11.74	11.74

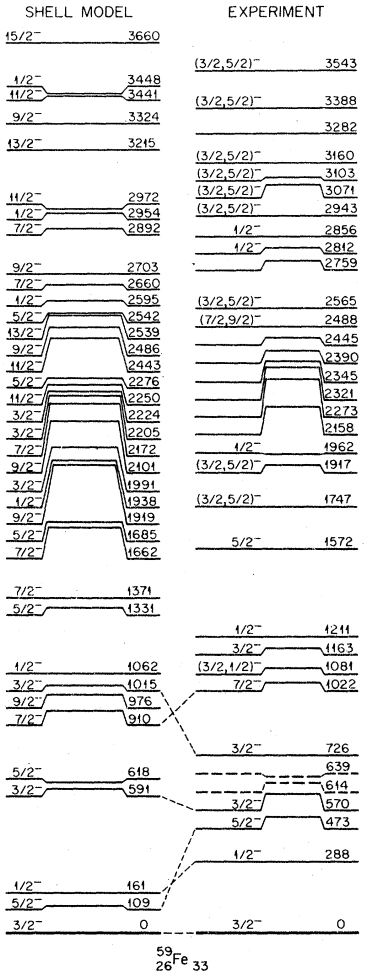

FIG. 4. Comparison between calculated (with the Vervier interaction) and experimentally known (Ref. 14) energy levels in ^{59}Fe. All energies are in keV.

Table III. Calculated energies (in MeV) of high-spin states in ^{59}Fe.

J^π	Vervier	J^π	Vervier
15/2$^-$	3.66	21/2$^-$	5.92
	4.92		6.87
17/2$^-$	4.29	23/2$^-$	7.19
	4.99		8.29
19/2$^-$	5.38	25/2$^-$	9.44
	5.51		9.89

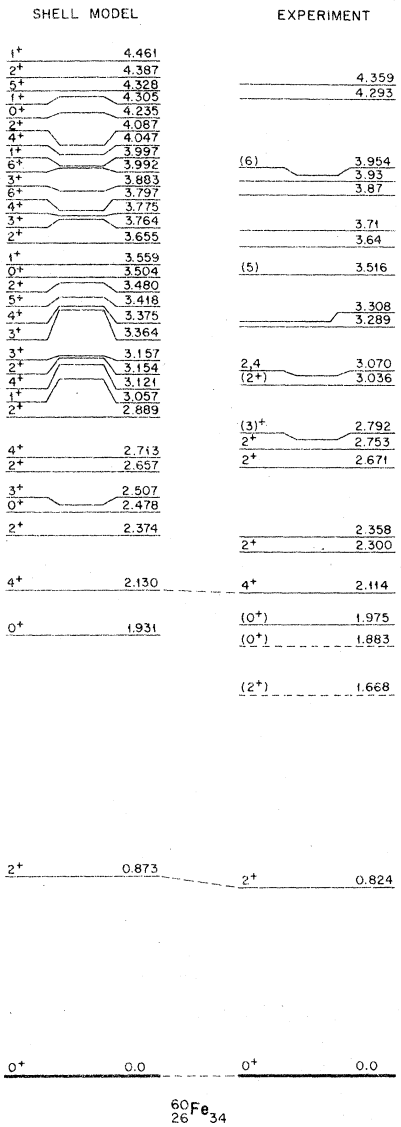

FIG. 5. Comparison between calculated (with the Vervier interaction) and experimentally known (Ref. 14) energy levels in ^{60}Fe. All energies are in MeV, because several experimentally known levels above 3.0 MeV have energy uncertainties exceeding 10 keV.

TABLE IV. Calculated energies (in MeV) of high-spin states in ^{60}Fe.

J^π	Vervier	J^π	Vervier
6$^+$	3.80	10$^+$	7.06
	4.00		7.23
7$^+$	5.43	11$^+$	8.35
	5.73		9.60
8$^+$	5.44	12$^+$	8.67
	6.04		9.76
9$^+$	6.37	13$^+$	12.27
	7.25		

Thus, in summary, the shell-model calculations of the $^{56-60}$Fe isotopes account for the systematic behavior of the excitation energies of low-lying levels quite well. The data for ^{59,60}Fe are too sparse for meaningful comparisons. There are predicted a number of high-spin states at relatively low excitation energies. For those cases where such levels are observed, the agreement is good enough to give confidence that there should be experimental analogs of these calculated states within 200-400 keV of the predicted positions.

IV. CALCULATIONS OF ELECTROMAGNETIC OBSERVABLES

A. Effective operators

We next discuss the calculation of electromagnetic observables in these nuclei. We consider only M1 and E2 observables since the model space does not allow any parity changing transitions and there is little, if any, data on transitions of higher multipolarity. In the calculation of electromagnetic observables the usual approach in shell-model technology is to use effective operators to include effects not explicitly included in the shell-model calculations such as core polarization. In the model space used here, the effective operators in principle should be those appropriate for ^{49}Ca and ^{49}Ti. Since we deal with nuclei rather far from the closed shell, it is perhaps more appropriate to choose operators which fit observed data in nuclei nearer in mass to the system we treat, and then see if these same operators fit the observed data in the Fe isotopes. Therefore, we first considered the isotopes ^{58}Ni and ^{54}Fe in model spaces completely analogous to the one used for the Fe isotopes. Thus, ^{58}Ni is two neutrons in the $f_{5/2}$, $p_{3/2}$, and $p_{1/2}$ neutron orbits, with a closed $f_{7/2}^8$ proton shell. The ^{54}Fe nucleus is treated as six protons in the $f_{7/2}$ shell. We assume state-independent effective one-body operators, and use harmonic oscillator wave functions with the oscillator parameters determined from the relation $\hbar\omega = 41\ A^{1/3}$. We thus assume one effective neutron charge for all neutron transitions, and one effective proton charge for all proton transitions. If we define the effective charges to be those which reproduce the observed B(E2) values for the transition from the first 2^+ to the ground state in ^{58}Ni and ^{54}Fe, respectively, we obtain the following effective charges:

$$\epsilon_n = 1.9\ e, \text{ and } \epsilon_p = 1.2\ e.$$

Therefore, the total proton charge employed in our calculations is 2.2 e. Both these effective charges are significantly larger than those found for the closed-shell nuclei ^{16}O and ^{40}Ca, where values less than 0.5 e are found.

We derive information about the effective M1 operator from information on magnetic moments in this mass region. For the $f_{7/2}$ proton orbit, there are measured magnetic moments for the lowest 2^+ and 6^+ states in ^{54}Fe. In our model space, these wave functions are pure $|f_{7/2}^6, J\rangle$ states. We list here, in units of nuclear magnetons (μ_N), the measured μ values[16] and the values calculated with the bare nucleon magnetic moment operator:

J^π	μ Calculated	μ Measured
2_1^+	+3.32	+(2.86 ± 0.56)
6_2^+	+9.96	±(8.22 ± 0.18)

This suggests that the effective M1 operator for the $f_{7/2}$ proton orbit in our model space is roughly state independent, and it is quenched by about 15% with respect to the bare operator. There are a number of measured magnetic moments in the Ni isotopes. In a recent paper by Hass, et al.,[17] the measured magnetic moments of the ground states of ^{57,59,61,63}Ni and of the first 2^+ states in ^{58,60,62}Ni are summarized. There is a strong suppression of the observed moments with respect to the Schmidt values for the isotopes with $A \leq 61$, while the observed values agree roughly with the Schmidt values for the isotopes with $A \geq 62$. All the observed moments are well reproduced by a calculation[17] in which one-particle excitations from the $f_{7/2}$ shell are included. The bare M1 operator has the form

$$M1 = \bar{\ell} + \mu_p \bar{\sigma}_p + \mu_n \bar{\sigma}_n .$$

The matrix element of the $\bar{\sigma}$ operator is large for the spin-flip transition $(j = \ell + \frac{1}{2}) \rightarrow (j = \ell - \frac{1}{2})$. These results are consistent with saying as long as there are $f_{5/2}$ neutron holes, there is a large contribution from states where an $f_{7/2}$ neutron is excited to the $f_{5/2}$ orbit. When the $f_{5/2}$ orbit is starting to fill, around A = 62, the core-excitation effect is quenched, and the Schmidt value is reproduced. No one has successfully reproduced this trend in the data with a constant, state-independent effective M1 operator acting in a pure $(p_{7/2}, f_{5/2}, p_{1/2})^{A-56}$ model for the Ni isotopes. (For a report of one effort, see Ref. 18). Thus, if M1 transitions are important in the Fe isotopes, we can anticipate some difficulty in reproducing the data with the bare M1 operator.

We have made several simple calculations to see if one-particle excitations of the $f_{7/2}$ shell have strong effects on the E2 observables in ^{54}Fe and ^{58}Ni. For ^{54}Fe we include configurations $f_{7/2}^{14}$ and $f_{7/2}^{13}\,(p_{3/2}, p_{1/2}, f_{5/2})^1$ and for ^{58}Ni we include the configurations $f_{7/2}^{16}\,(p_{3/2}, p_{1/2}, f_{5/2})^2$ and $f_{7/2}^{15}\,(p_{3/2}, p_{1/2}, f_{5/2})^3$. For the two-body interaction, we employ the Kuo-Brown interactions derived[19] from the Hamada-Johnston potential for use in shell-model calculations with a ^{40}Ca core and particles in the (fp) shell. Thus, the interaction is not appropriate for the model space. The question we ask is, "does including $f_{7/2}$ excitation introduce large changes in the calculated E2 transitions?". For this purpose, the interaction is probably adequate. The single-particle energies are selected so that the observed spectrum of ^{57}Ni is roughly reproduced in the space $f_{7/2}^{16}\,(p_{3/2}, p_{1/2}, f_{5/2})^1$. We then do a series of calculations in which the $f_{7/2}$ orbit is varied with respect to the $p_{3/2}$, $p_{1/2}$, and $f_{5/2}$ orbits in such a way as to vary the amount of 1p-1h excitation of the $f_{7/2}^{16}$ configuration from 10%-35%. In these calculations, we assume the same state-independent, effective charge for neutrons and protons, i.e., $\epsilon_n = \epsilon_p = 1.0$ e. We use the bare M1 operator to calculate the magnetic moments in iron and nickel isotopes in the same model spaces. In Table V we show the calculated results for the B(E2) for the first 2^+ to ground state in ^{54}Fe and ^{58}Ni, the magnetic moment for the first 2^+ states in ^{54}Fe and ^{58}Ni, and the magnetic moment for the ground state of ^{57}Ni.

We see that in all cases the inclusion of core excitation leads to distinct improvement in the calculated observables. For the magnetic moments, these results are consistent with Hass, et. al.,[17] for the Ni isotopes, i.e., the only new result here is that for the magnetic moment of ^{54}Fe. For the E2 transitions, it is possible to reproduce, at least qualitatively, the observed data in both ^{54}Fe and ^{58}Ni with similar neutron and proton effective charges. (These E2 results are consistent with the results of Glaudemans, et. al.,[20] which were received as this manuscript was in preparation.)

One can expect difficulties in using state-independent effective operators in the calculations of the iron isotopes reported here, particularly for M1 observables. The M1 observables are strongly affected by core-excitation effects which we omit from the calculations, and the core-excitation effects vary significantly from nucleus to nucleus, in large measures because of Pauli blocking effects. In other words, the effects we would try to mock up with a state-independent operator are strongly state dependent. A lengthier discussion of these and related problems is presented by Pasquini and Zuker.[21]

B. E2 Observables in ground-state bands of ^{56,58,60}Fe

We first compare E2 transition strengths for the decay of the lowest 2^+ state to the ground state in the three even-even isotopes ^{56,58,60}Fe. In Table VI are shown the values calculated with the two sets of effective charges. In one case we used $\epsilon_p = 1.2$ e, $\epsilon_n = 1.9$ e for reasons discussed above. In the second case we used $\epsilon_p = \epsilon_n = 1.0$ e. There are large discrepancies if we use the effective charges suggested by the E2 transitions in ^{54}Fe and ^{58}Fe (i.e., column A). From measurements, the E2 strength for this transition remains roughly constant as a function of the mass number, while the calculated value increases by 70% between ^{56}Fe and ^{60}Fe. There is significant improvement if the effective charges are reduced to $\epsilon_p = \epsilon_n = 1.0$ e. In this case, the calculated values are roughly comparable with experiment, and the increase in this strength as a function of the mass number is significantly less.

Also shown in Table VI are the calculated B(E2) values for transitions between members of what might be identified as ground-state bands in ^{56,58,60}Fe. There is a particularly interesting feature in this experimental data which has been commented on pre-

Table V. Selected M1 and E2 observables in ^{54}Fe, ^{57}Ni, and ^{58}Ni. For E2 observables an added effective charge of 1.0 e is used for both neutrons and protons. For M1 observables, the bare M1 operator is used. The columns headed "% Core excitation" show results calculated in model spaces when the indicated percentage of the wave function is made up of wave functions with one particle excited from the $f_{7/2}$ shell.

Nucleus	Operator	Experiment[a]	Calculation % Core excitation 0%	15%	25%	35%
^{54}Fe	B(E2) $2_1^+ \rightarrow 0_1^+$ (e^2fm^4)	(128 ± 10)	98	150	160	190
	2_1^+ Magnetic moment (μ_N)	+(2.86 ± 0.56)	+3.32	+2.74	+2.64	+2.44
^{57}Ni	$3/2_1^-$ Magnetic moment (μ_N)	±(0.88 ± 0.06)	-1.92	-0.92	-0.68	-0.37
^{58}Ni	B(E2) $2_1^+ \rightarrow 0_1^+$ (e^2fm^4)	(139 ± 5)	42	97	113	139
	2_1^+ Magnetic moment (μ_N)	-(0.06 ± 0.12)	-0.31	-0.27	-0.19	-0.02

[a]The B(E2) values are from S. Raman, W. T. Milner, C. W. Nestor, Jr., and P. H. Stelson, Contributed paper, Proceedings of the International Conference on Nuclear Structure (Organizing Committee of the Tokyo Conference, 1977) p. 79 and to be published. The magnetic moments are from Ref. 16.

viously.[7] If one identifies as states in a rotational band those states which are connected by strong E2 transitions, then the 6^+ member of the ground-state band in ^{56}Fe is the second 6^+ state, and not the lowest one, so that there is something like a band crossing in this nucleus at the 6^+ level. This feature, and the other qualitative features of the relative B(E2) strengths in the ground-state band of ^{56}Fe are reproduced by the shell-model calculations, as was observed previously.[7] In ^{58}Fe, a similar structure seems to exist (certainly in the calculations but also suggested by the measurements) but here the "crossing" occurs at the 8^+ level. This shift is also reproduced by the calculations.

The quadrupole moment of the first 2^+ state in ^{56}Fe is known[16] to be -(24 ± 3) e fm^2, in excellent agreement with the value of -20 e fm^2 which is calculated with $\epsilon_p = \epsilon_n = 1.0$ e. A value of +(29 ± 8) e fm^2 for the quadrupole moment in ^{58}Fe has been reported.[22] This value is in sharp disagreement with the calculated (with $\epsilon_p = \epsilon_n = 1.0$ e) value of -21 e fm^2. The reported measured value was used[8] to infer a rather abrupt shape change between ^{56}Fe and ^{58}Fe. However, experimental problems were found in the ^{58}Fe measurement, and the work has not been published formally. As indicated previously,[4] a measurement of this number would be of significant interest.

In summary, the E2 observables for many observed E2 properties for the "ground-state bands" in ^{56}Fe, ^{58}Fe, and ^{60}Fe are reproduced extremely well by the shell-model calculations. The relative B(E2) values for these transitions are insensitive to the assumed effective charges. The absolute values suggest that the effective neutron charge in ^{56,58,60}Fe is significantly smaller than that implied by a comparison of theory and experiment for ^{58}Ni. A more extended discussion of the "band" structure in these nuclei is given below.

C. Branching ratios

There exists considerable data on branching ratios for the decay of excited states in ^{56}Fe, ^{58}Fe, and ^{60}Fe. The branching ratios are, of course, functions of the transition energies and the transition matrix elements. In calculating branching ratios, we use the measured decay energies as opposed to the calculated ones. Thus, any discrepancy arises from inaccuracies in the calculated matrix elements, and not from energy discrepancies. In the calculations discussed here, E2 matrix elements are calculated with $\epsilon_p = \epsilon_n = 1.0$ e. The M1 matrix elements are calculated with the free-nucleon operator.

In Table VII the calculated and observed branching ratios for the decay of three excited states in ^{56}Fe are shown. The table also shows the calculated E2 and M1 widths in electron volts. There is reasonable agreement for the branching ratios in the decay of the 6_2^+ and 7_1^+ states. There is an inversion of strength for the decay of the 8_1^+ state. This defect is not present in the calculations made with the Horie-Ogawa interaction as discussed by Bendjaballah, et al.[5] For the 6_2^+ and 7_1^+ states, the calculated branching ratios would be in qualitative agreement with experiment if M1 contributions were ignored. However, the calculated M1 strength dominates the E2 strength for the decay of the 7_1^+ state. There is a rather strong M1 branch calculated for the 8_1^+ state, but not seen experimentally. States in ^{56}Fe can be considered approximately as ^{54}Fe states coupled to ^{58}Ni states. Recall that the neutron M1 operator was quenched by core-excitation

TABLE VI. B(E2) values for transitions between low-lying levels in ^{56}Fe, ^{58}Fe and ^{60}Fe. The column headed "A" shows results calculated with the added effective charges ϵ_n = 1.9 e and ϵ_p = 1.2 e. The column headed "B" shows results calculated with added effective charges of 1.0 e for neutrons and protons. The symbol "n.c." denotes not calculated.

		$B(E2)_{i\to f}$ (e^2fm^4)		
		Calculation		Experiment[a]
Nucleus	$J_i^\pi \to J_f^\pi$	A	B	
^{56}Fe	$2_1^+ \to 0_1^+$	360	176	206 ± 10
	$4_1^+ \to 2_1^+$	457	224	295 ± 79
	$6_1^+ \to 4_1^+$	57	32	56^{+43}_{-29}
	$6_2^+ \to 4_1^+$	361	176	250 ± 43
	$8_1^+ \to 6_1^+$	n.c.	12	55 ± 7
	$8_1^+ \to 6_2^+$	n.c.	103	60 ± 11
^{58}Fe	$2_1^+ \to 0_1^+$	515	226	180 ± 10
	$4_1^+ \to 2_1^+$	571	223	740^{+310}_{-170}
	$6_1^+ \to 4_1^+$	n.c.	262	205 ± 23
	$8_1^+ \to 6_1^+$	n.c.	10	33 ± 15
	$8_1^+ \to 6_2^+$	n.c.	37	92 ± 36
	$8_2^+ \to 6_1^+$	n.c.	174	
^{60}Fe	$2_1^+ \to 0_1^+$	598	239	186 ± 38
	$4_1^+ \to 2_1^+$	787	311	190^{+63}_{-38}

[a]The B(E2) values for the 2_1^+ states are from S. Raman, W. T. Milner, C. W. Nestor, Jr., and P. H. Stelson, Contributed paper, Proceedings of the International Conference on Nuclear Structure (Organizing Committee of the Tokyo Conference, 1977) p. 79 and to be published. The remaining B(E2) values for ^{56}Fe, ^{58}Fe, and ^{60}Fe are from Refs. 7, 8, and 3, respectively.

effects in ^{58}Ni. Thus, one should be concerned that the large M1 contributions in the calculations for ^{56}Fe are spurious.

In Table VIII, the calculated and observed branching ratios of M1 and E2 widths for the decays of four states in ^{58}Fe are shown. With the exception of the decay of the 4_2^+ state, the theory-experiment agreement is quite unsatisfactory. The M1 widths are crucial in almost all of these decays. If the M1 strengths for the decays of the 2_2^+ and 3_1^+ states were significantly quenched, there could be reasonable agreement for the branching ratios in these nuclei. On the other hand, the agreement for the 4_2^+ branching depends on the large M1 widths, and there is a suggestion they should be slightly larger. For the 5_1^+ decay, one would need to have the large M1 width to the 4_2^+ state instead of to the 4_1^+ state. All this assumes that the E2 strengths are accurate in the calculations, a very strong assumption. But it is obvious that no overall state-independent renormalization of the M1 strength can lead to good agreement for the branching ratios in ^{58}Fe.

TABLE VII. Branching ratios in ^{56}Fe. In these calculations an added effective charge of 1.0 e is used for neutrons and protons. The bare M1 operator is used to calculate magnetic contributions.

	Calculation		Branching Ratio (%)	
$J_i^\pi \to J_f^\pi$	Γ(E2) (eV)	Γ(M1) (eV)	Calculation	Experiment[a]
$6_2^+ \to 4_1^+$	0.19×10^{-2}		91	78 ± 4
$\to 4_2^+$	0.33×10^{-6}		0	
$\to 6_1^+$	0.34×10^{-6}	0.18×10^{-3}	9	22 ± 4
$7_1^+ \to 6_1^+$	0.27×10^{-3}	0.20×10^{-1}	93	82 ± 3
$\to 6_2^+$	0.99×10^{-5}	0.16×10^{-2}	7	18 ± 3
$8_1^+ \to 6_1^+$	0.22×10^{-3}		19	73 ± 4
$\to 6_2^+$	0.64×10^{-3}		57	27 ± 4
$\to 7_1^+$	0.25×10^{-6}	0.25×10^{-3}	23	

[a]From Ref. 7.

Table IX shows the calculated and observed branching ratios for the decay of the 2_2^+ and 3_1^+ states in ^{60}Fe. For each of these cases, the M1 widths dominate the calculated branching ratios, and there is generally poor agreement with experiment. If the M1 spectra were strongly quenched, the E2 transitions by themselves would account for the branching ratios of the 2_2^+ state, but the calculations imply that the M1 transitions are too weak for the decay of the 3_1^+ state.

We conclude that in the absence of a usable effective M1 operator for the model space we employ, the model is inadequate for a meaningful calculation of branching ratios where competition between M1 and E2 is possible.

V. "BAND STRUCTURE" IN THE EVEN-IRON ISOTOPES

There is agreement between theory and experiment that there are enhanced E2 transitions between the lowest 0^+, 2^+, and 4^+ states in the isotopes ^{56}Fe, ^{58}Fe, and ^{60}Fe. This behavior is suggestive of a rotational behavior, and it raises the question of the character of the collective behavior of other states in the low-lying spectrum of these isotopes. Since there is no unambiguous experimental data

TABLE VIII. Branching ratios in ^{58}Fe. In these calculations an added effective charge of 1.0 e is used for neutrons and protons. The bare M1 operator is used to calculate magnetic contributions.

	Calculation		Branching Ratio (%)	
$J_i^\pi \to J_f^\pi$	Γ(E2) (eV)	Γ(M1) (eV)	Calculation	Experiment[a]
$2_2^+ \to 0_1^+$	0.64×10^{-4}		9	42 ± 7
$\to 2_1^+$	0.22×10^{-4}	0.18×10^{-3}	91	58 ± 9
$3_1^+ \to 2_1^+$	0.11×10^{-4}	0.39×10^{-5}	39	67 ± 10
$\to 2_2^+$	0.54×10^{-5}	0.18×10^{-4}	60	33 ± 5
$4_2^+ \to 2_1^+$	0.86×10^{-3}		66	43 ± 7
$\to 2_2^+$	0.40×10^{-4}		3	9 ± 4
$\to 4_1^+$	0.48×10^{-6}	0.36×10^{-3}	27	35 ± 6
$\to 3_1^+$	0.20×10^{-5}	0.40×10^{-4}	3	13 ± 2
$5_1^+ \to 4_1^+$	0.38×10^{-5}	0.12×10^{-3}	77	weak
$\to 3_1^+$	0.30×10^{-4}		19	31 ± 5
$\to 4_2^+$	0.14×10^{-6}	0.60×10^{-5}	4	69 ± 11

[a]From Ref. 8.

TABLE IX. Branching ratios in ^{60}Fe. In these calculations an added effective charge of 1.0 e is used for neutrons and protons. The bare M1 operator is used to calculate magnetic contributions.

	Calculation		Branching Ratio (%)	
$J_i^\pi \to J_f^\pi$	Γ(E2) (eV)	Γ(M1) (eV)	Calculation	Experiment[a]
$2_2^+ \to 0_1^+$	0.28×10^{-3}		13	55 ± 8
$\to 2_1^+$	0.26×10^{-3}	0.16×10^{-2}	86	45 ± 6
$3_1^+ \to 2_1^+$	0.12×10^{-6}	0.13×10^{-3}	43	72 ± 5
$\to 4_1^+$	0.25×10^{-5}	0.17×10^{-3}	56	3 ± 1
$\to 2_2^+$	0.58×10^{-8}	0.26×10^{-5}		25 ± 2

[a]From E. B. Norman, C. N. Davids, M. J. Murphy, and R. C. Pardo, Phys. Rev. C 17, 2156 (1978).

about E2 transitions between the higher spin states in these isotopes, we have treated the calculated B(E2) values as "experimental" data, and we have studied these data for "evidence of collective behavior". To do this, we collected all the "data" on strong B(E2) values (strong here is $\geq$ 100 e^2 fm^4) and looked for sets of states connected by strong transitions. There are a number of such transitions outside the so-called ground-state bands, but we could find no clear pattern in ^{56}Fe and ^{58}Fe. In the case of ^{60}Fe, there does appear in the calculations a set of states which are strongly coupled and which are not coupled to the "ground-state band" states. We have attempted to summarize this in Table X. We show there the ground-state bands [defined as the lowest even J states for J > 4 which are coupled to the lowest J = 0, 2, and 4 states by strong E2 transitions], and indicate for the states in this band the B(E2) values and the static quadrupole moments. We have also looked further to the question of whether these nuclei are truly rotational. In particular, can the calculated properties be reproduced by a common rotational model prescription that the wave function can be written as the product of a deformed instinsic state, χ times an element of the rotation matrix $D_{KM}(\theta,\phi)$, i.e.,

$$\psi_M^J = D_{KM}^J \chi_K .$$

In this model the static quadrupole moment is related to the quadrupole moment of the intrinsic state through the relation

$$Q_J^2 = \frac{3K^2 - J(J+1)}{(J+1)(2J+3)} Q_0 .$$

If we assume this prescription and a given value of K, we can calculate the intrinsic quadrupole moment, Q_0, from the static moment. In Table X we give the intrinsic quadrupole moment implied by the static moment and the assumption that K = 0.

Consider first the ground-state "band", i.e., those states beginning with the ground state which are connected by large E2 matrix elements. There is a very similar pattern for all three isotopes. There is a set of positive parity states with J = 0, 2, 4, 6, and 8 in all isotopes which have large connecting B(E2) values, and which are characterized by a quadrupole moment which implies a prolate shape. If we assume that each state is a projection from an intrinsic state, as defined above, then we see a strong diminution in the intrinsic moment as one moves up the ground-state band in J. There is no state above the 8^+ state in any of the three calculations which has a strong B(E2) to the 8^+ state of the ground-state band. In all three cases, one or two members of the ground-state band are not the yrast levels, so there is something akin to a "band crossing". In all three cases, for transitions involving states with J $\geq$ 6, the ratio of the calculated B(E2) to the B(E2) calculated from the $2_1^+ \to 0_1^+$ transition is considerably reduced vis-a-vis the rotational model prediction. Thus, except for the high degree of E2 collectivity, there is little relation between the shell-model result and a picture of states projected from a single intrinsic state. Parikh[23] has reported on some Hartree-Fock calculations in this mass region. He finds that the lowest oblate and prolate states are almost degenerate. This is consistent with our results.

TABLE X. Electric quadrupole observables in ^{56,58,60}Fe "Bands". All observables are calculated with an added effective charge of 1.0 e for neutrons and protons. Q_0 is intrinsic quadrupole moment as defined in the text.

^{56}Fe			^{58}Fe			^{60}Fe		
J_i^π	$B(E2)_{J\to J-2}$ (e^2 fm^4)	Q_0 (e fm^2)	J_i^π	$B(E2)_{J\to J-2}$ (e^2 fm^4)	Q_0 (e fm^2)	J_i^π	$B(E2)_{J\to J-2}$ (e^2 fm^4)	Q_0 (e fm^2)
0_1^+			0_1^+			0_1^+		
2_1^+	176	-26	2_1^+	226	-27	2_1^+	239	-29
4_1^+	224	-29	4_1^+	233	-25	4_1^+	311	-34
6_2^+	176	-18	6_1^+	262	-24	6_2^+	187	-30
8_1^+	103	-4	8_2^+	174	-3	8_3^+	46	-5
						0_2^+		
						2_2^+	136	16
						6_1^{+a}		15
						8_1^+	137	35
						10_1^+	149	46
						12_1^+	95	53

[a]There is no obvious candidate for the 4^+ member of the second band from the calculations.

For the first even-J states outside the ground-state band, there is no strong pattern for ^{56}Fe and ^{58}Fe. For both nuclei, the quadrupole moments for the highest spin values suggest an oblate shape. For ^{60}Fe, there is a suggestion of a pattern. There are relatively large B(E2) values for the 6^+, 8^+, 10^+, and 12^+ states. These are summarized in Table X. In addition, all these states have quadrupole moments consistent with an oblate deformation, where the implied intrinsic moment increases in size as the spin increases. In a finite dimensional shell-model space, the highest spin state is that obtained by putting the particles in the highest allowed m state. In the model space treated here, the highest spin state occupied by the protons is a 6^+ state. The quadrupole moment is the expectation value of the Q^2 operator in the state M = J. Thus, for J = 6, the protons are aligned as much as possible with the Z axis, i.e., the particles are in the (j,m) = (7/2,7/2) and (7/2,5/2) states, respectively. Thus, the motion of the particle is predominantly in the plane perpendicular to the Z axis, i.e., strongly oblate. The calculations imply that the neutrons align themselves in this way as much as possible. As the number of neutrons increases, there seems to be a tendency for the particles to align to give oblate deformations at lower J values. There is an interesting pattern in the intrinsic quadrupole moments of the yrast states in ^{60}Fe. For the lowest J values, the intrinsic moments are large prolate, and they decrease in size as J increases. Then as J goes beyond 6, the yrast levels have oblate intrinsic moments which increase as J increases to a maximum for the highest spin J = 12 state. If there is any physical significance to these intrinsic moments, a picture is suggested of a very soft rotating nucleus which starts out in a prolate configuration at the lowest spin, and "anti-stretches" with increasing J. There is then a band crossing, and the centrifugal force gradually changes the shape to produce an increasingly oblate nucleus. The pattern is obviously suggestive of the behavior, proposed by the Copenhagen school,[24] of strongly deformed nuclei at very high angular momentum.

In Fig. 6 the calculated eigenvalues of the lowest six states of each spin are plotted as a function of J(J+1). The states which are coupled strongly to the ground state by E2 transitions are connected by a solid line. All these states have prolate static quadrupole moments. The even-J, yrast levels with $J \geq 6$ are connected by a dashed line. This line is very straight, suggestive of a good rotor. If it is projected back to low spin, it comes very close to the 2_2^+ state which also has a reasonably large oblate quadrupole moment. This state has a strong decay to the 0_2^+ level. This plot suggests a classic band-crossing solution. There appears to be a distinct oblate band which mixes rather strongly with the prolate band states at J = 4 and J = 6 but which is relatively pure above J = 6. One could hope that with higher energy heavy-ion beams, the probability of populating the 12^+ and 10^+ members of this oblate part of the yrast spectrum will be large enough that one might study these levels.

VI. SUMMARY OF RESULTS

We have summarized here in some detail conventional shell-model calculations of the iron isotopes, insofar as excitation energies and electromagnetic properties are concerned. To the extent that there is information on the position of high-spin states in these nuclei, the calculations are in reasonable agreement with experiment. In general, the calcula-

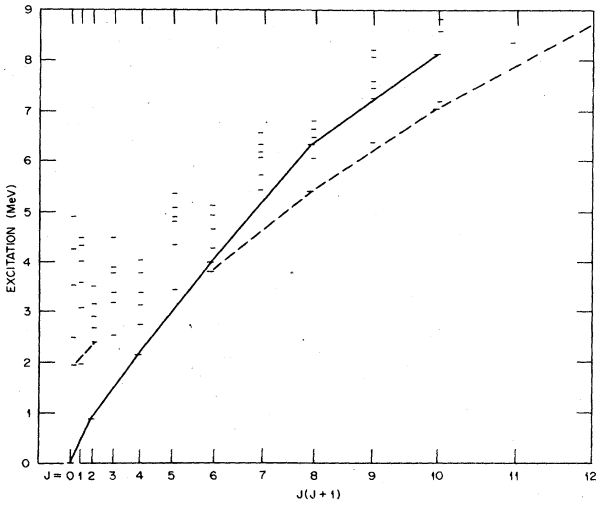

FIG. 6. The calculated excitation energies, in MeV, of the lowest six eigenvalues in ^{60}Fe corresponding to positive parity states with spins from J=0 to J=12 plotted as a function of J(J+1). The solid line joins all states starting from the ground state which are connected by strong E2 transitions. The dashed line joins a separate set of states connected by similarly strong E2 transitions.

tions are in striking agreement with experiment for the lowest 3 MeV of excitation.

The calculations of the B(E2) and B(M1) values for transitions involving low-lying states in these nuclei depend very critically on the effective operators which are used in the calculations. There is a large difference between the neutron effective charges needed in the Ni isotopes in a closed $f_{7/2}$ shell model and those needed in the Fe isotopes. We have checked the importance of single-particle excitations from the $f_{7/2}$ shell to the $p_{3/2}$, $p_{1/2}$, and $f_{5/2}$ shells in calculations of ^{54}Fe and ^{58}Ni. The effects are much stronger in ^{58}Ni. The difference presumably reflects the fact that in ^{54}Fe, in lowest order $(\pi f_{7/2}^{-2})$, there are proton decays allowed, while in ^{58}Ni, in lowest order, there are no contributions from the proton. Thus, proton excitations in ^{58}Ni should make a larger change in B(E2) calculations. We have found that the $f_{7/2}$ hole excitations not only lead to better agreements for calculations of the magnetic moments of the Ni isotopes as previously reported, but that they also give shifts in the right direction for the 2^+ and 6^+ states in ^{54}Fe.

When we use effective charges arbitrarily chosen to fit the magnitude of the B(E2) values in ^{56}Fe and ^{58}Fe for the $2_1^+ \rightarrow 0_1^+$ transitions, we find that the measured relative B(E2) values for the transitions in the ground-state bands are rather well accounted for by the calculations. The measured branching ratios are very poorly reproduced by the calculations. This is due, in large measure, to the strong state dependence of the effective M1 operator which is known to exist for the Ni isotopes. We can offer no simple fix for this discrepancy. The explicit inclusion of $f_{7/2}$ excitations in the calculations leads to prohibitively large matrices for $^{58\text{-}60}$Fe.

The calculations show no evidence for a sudden shape transition for the ground-state band between ^{56}Fe and ^{58}Fe. In the absence of any confirmation of the change in the quadrupole moment of the lowest 2^+ state in these isotopes, there is no experimental evidence for the change either. There is evidence of an interesting phase change in the yrast levels of ^{60}Fe. The yrast states for J = 0, 2, 4 are prolate, while for J = 6, 8, 10, and 12, they are oblate. The shell model has a long history of successfully describing yrast levels for low-spin states, so that there is reasonable expectation that the high-spin yrast states described here for ^{60}Fe have some reasonable analog experimentally.

The previously reported results of Parikh,[23] and the results summarized here suggest that a single rotational model is not applicable for these normal parity states. Several authors[7,13,25,26] have suggested that an aligned-coupling scheme may be more applicable. A discussion of the calculation of the even-iron isotopes ^{56,58,60}Fe in an aligned-coupling scheme will be published in a subsequent paper.

ACKNOWLEDGMENTS

We thank D. C. Larson who participated in the early stages of this work. The present research was sponsored by the Divisions of Nuclear Physics and Nuclear Sciences, U.S. Department of Energy, under contract No. W-7405-eng-26 with the Union Carbide Corporation.

[1]J. B. McGrory, Phys. Rev. 160, 915 (1967).
[2]J. B. McGrory, Phys. Lett. 26B, 604 (1968).
[3]E. K. Warburton, J. W. Olness, A. M. Nathan, J. J. Kolata, and J. B. McGrory, Phys. Rev. C 16, 1027 (1977).
[4]A. M. Nathan, J. W. Olness, E. K. Warburton, and J. B. McGrory, Phys. Rev. C 17, 1008 (1978).
[5]N. Bendjaballah, J. Delaunay, T. Nomura, and H. J. Kim, Phys. Rev. Lett. 36, 1536 (1976).
[6]D. J. Sarantites, J. Urbon, and L. L. Rutledge, Jr., Phys. Rev. C 14, 1412 (1976).
[7] N. Bendjaballah, J. Delaunay, A. Jaffrin, T. Nomura, and K. Ogawa, Nucl. Phys. A284, 513 (1977).
[8]S. Cavallaro, J. Delaunay, R. Ballini, T. Nomura, N. Bendjaballah, and C. Tosello, Nucl. Phys. A293, 125 (1977).
[9]H. Verheul and R. L. Auble, Nucl. Data Sheets 23, 455 (1978).
[10]J. Vervier, Nucl. Phys. 78, 497 (1966).
[11]S. Cohen, R. D. Lawson, M. H. Macfarlane, S. P. Pandya, and M. Soga, Phys. Rev. 160, 903 (1967).
[12]J. B. French, E. C. Halbert, J. B. McGrory, and S. S. M. Wong, Advances in Nuclear Physics, edited by M. Baranger and E. Vogt (Plenum, New York, 1969), Vol. 3., p. 193.
[13]H. Horie and K. Ogawa, Nucl. Phys. A216, 407 (1973).
[14]The ^{56}Fe and ^{57}Fe level schemes are mainly from R. L. Auble, Nucl. Data Sheets 20, 253

(1977) and ibid. 20, 327 (1977), respectively. The ^{58}Fe scheme is from D. C. Kocher and R. L. Auble, ibid. 19, 445 (1976) and Ref. 8. The ^{59}Fe scheme is from H. J. Kim, ibid. 17, 485 (1976) and from K. C. McLean, S. M. Dalgliesh, S. S. Ipson, and G. Brown, Nucl. Phys. A191, 417 (1972). The ^{60}Fe scheme is from E. B. Norman, C. N. Davids, M. J. Murphy, and R. C. Pardo, Phys. Rev. C 17, 2176 (1978); E. B. Norman, C. N. Davids, and C. E. Moss, Phys. Rev. C 18, 102 (1978); Ref. 3 and Ref. 15. See also Ref. 16.

[15]M. Sakai, in Proceedings of the Symposium on In-Beam Spectroscopy with Heavy Ions, edited by H. Kamitsubo and T. Nomura, Institute of Physical and Chemical Research (Japan) Cyclotron Progress Report (1973), Supplement 2, p. 114.

[16]C. M. Lederer, V. S. Shirley, E. Browne, J. M. Dairiki, R. E. Doebler, A. A. Shihab-Eldin, L. J. Jardine, J. K. Tuli, and A. B. Buyrn, Table of Isotopes, Seventh Edition (John Wiley, New York, 1978). Appendix VII contains measured nuclear magnetic dipole moments and electric quadrupole moments.

[17]M. Hass, N. Benczer-Koller, J. M. Brennan, H. T. King, and P. Goode, Phys. Rev. C 17, 997 (1978).

[18]J. E. Koops and P. W. M. Glaudemans, Z. Physik A280, 181 (1977).

[19]T. T. S. Kuo, private communication.

[20]B. C. Metsch, A. S. M. van Hees, and P. W. M. Glaudemans, private communication.

[21]E. Pasquini and A. Zucker, in Proceedings of the Topical Conference on Physics of Medium-Light Nuclei, Florence, Italy, 1977 edited by P. Blasi and R. A. Ricci (Editrice Compositori, Bologna, 1978) p. 62.

[22]C. W. Towsley, Ph.D Thesis, Univ. Rochester (1974) unpublished. D. Cline, private communication.

[23]J. K. Parikh, Phys. Rev. C 10, 2568 (1974).

[24]A. Bohr and B. R. Mottelson, in Proceedings of the International Conference on Nuclear Structure, Tokyo, Japan, 1977, edited by T. Marumori (Physical Society of Japan, 1978) J. Phys. Soc. Japan Supplement 44, 157 (1978).

[25]K. H. Bhatt, J. C. Parikh, and J. B. McGrory, Nucl. Phys. A224, 301 (1974).

[26]V. Paar, Nucl. Phys. A185, 544 (1972).